

Analysis of a luminous signal with deterministic profile by using photon counting techniques.

Carla Recio Fernández

March 24, 2024

Abstract

Two different light beam signals, both with the same unknown period (P) and different unknown modulation factors (M), were studied and characterized using photon counting techniques. For the first signal, the obtained values were $\bar{M} = 0.501 \pm 0.007$ and $\bar{P} = 9.7 \pm 0.5$ ms. For the second signal, the values found were $\bar{M} = 0.738 \pm 0.014$ and $\bar{P} = 10.2 \pm 0.2$ ms.

1 Introduction

When studying optical signals, two main approaches are commonly used: frequency-domain analysis and time-domain analysis. In the time domain, signals are characterized by their intensity variations over time, often described by parameters such as the period P and the modulation factor M . A key aspect of this characterization is the statistical analysis of signal fluctuations, which can be quantified using the second-order factorial moment $n^{(2)}$. This parameter provides a more precise and stable measurement than standard deviation-based methods, as it captures the correlation between intensity variations within a given time interval T , sampling time.

Since direct measurement of instantaneous intensity is often impractical, photon-counting techniques are employed to integrate the intensity over a finite sampling period. The measured quantity, $W(t, T)$, represents the intensity integrated over time and is given by:

$$W(t, T) = \int_t^{t+T} I(t') dt' \quad (1)$$

where $I(t)$ is the time-dependent intensity of the signal. To quantify fluctuations in the signal, the second-order factorial moment is defined as:

$$n^{(2)} = \frac{\langle W(t, T)^2 \rangle}{\langle W(t, T) \rangle^2} = 1 + \frac{Var(W)}{\langle W \rangle^2} \quad (2)$$

where $\langle W \rangle$ is the mean value of W , and $Var(W)$ represents its variance. The value of $n^{(2)}(T)$ provides insights into the degree of fluctuation in the signal:

- If $n^{(2)}(T) = 1$, the signal is constant over the time, indicating no fluctuations.
- If $n^{(2)}(T) > 1$, the signal exhibits some degree of fluctuation.
- If $n^{(2)}(T) \gg 1$, the fluctuations are significant, meaning there is a strong variation between the maximum (A_1) and the minimum (A_2) intensity levels.

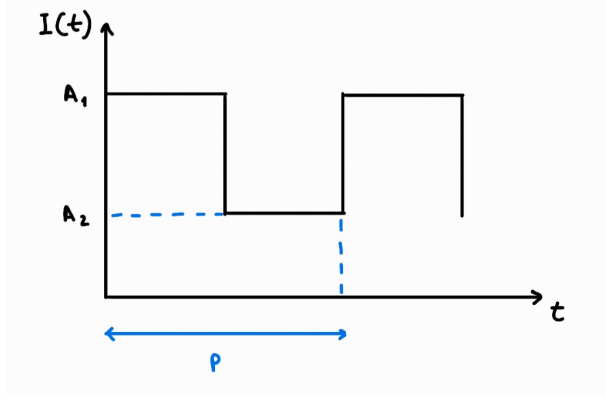


Figure 1: Schematic representation of a square wave signal over time, showing the period P and the maximum (A_1) and minimum (A_2) intensity levels.

For a time-modulated signal with a square profile as shown in Figure 1, where the intensity alternates between two values,

$$I(t) = \begin{cases} A_1 & \text{if } 0 \leq t \leq P/2 \\ A_2 & \text{if } P/2 \leq t \leq P \end{cases} \quad (3)$$

the second-order factorial moment can be expressed in terms of the modulation factor M , the period P , and the sample time T :

$$n^{(2)} = \begin{cases} (1 - \frac{4T}{3P})M^2 + 1 & \text{if } 0 \leq T \leq P/2 \\ (\frac{4T}{3P} - \frac{P^2}{3T^2} + \frac{2P}{T} - 3)M^2 + 1 & \text{if } P/2 \leq T \leq P \end{cases} \quad (4)$$

where the modulation factor M is defined as:

$$M = \frac{A_1 - A_2}{A_1 + A_2} \quad (5)$$

which quantifies the contrast between the two intensity levels of the signal. By analysing the dependence of $n^{(2)}(T)$ on the modulation factor and the sampling time, different fluctuation regimes can be identified, providing information about the properties of the optical signal. This dependency can be observed in the following representation of the explained theoretical model:

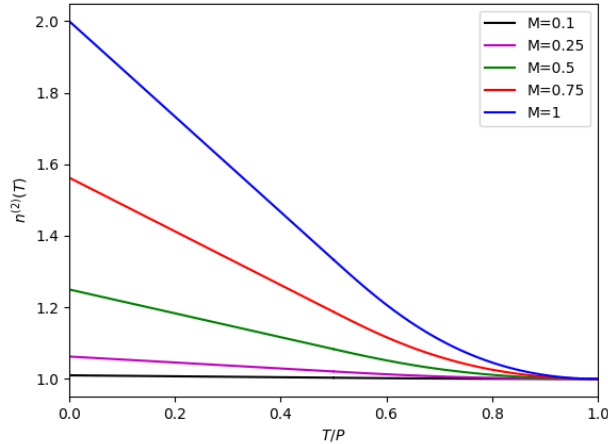


Figure 2: Theoretical model of the second-order factorial moment for different values of M as a function of the ratio T/P .

In this work, we aim to characterize a time-modulated optical signal with a deterministic square profile using photon-counting techniques. By measuring the second-order factorial moment and the modulation factor, we will quantify the signal fluctuations and establish a theoretical model to describe its statistical properties.

2 Experimental procedure

First, in order to characterise the light pulses, the following setup is used:

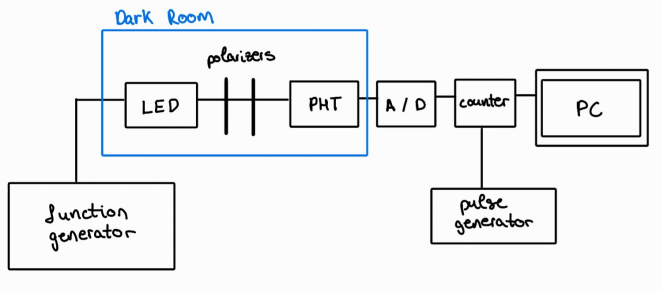


Figure 3: Schema of the experimental set up, where *PHT* is the photomultiplier and *A/D* is the amplifier and the discriminator.

The system begins with a function generator, which produces a square-wave voltage signal to drive the LED. The pulsed light passes through a series of polarizers inside a dark room, so that stray light was minimized, before reaching the photomultiplier (*PHT*). The photomultiplier serves as the primary detector, converting incident photons into measurable electrical pulses via a cascade of electron multiplication. The raw signal from the photomultiplier is inherently noisy due to secondary effects such as thermal electron emission and collisions with residual gas molecules in the tube.

To isolate valid pulses, the signal is first amplified (with the amplifier) and then processed by a discriminator (*A/D*). This component filters out signals by enforcing strict voltage thresholds, ensuring only pulses of the expected amplitude are counted. The discriminator's voltage window was calibrated to reject low-amplitude noise, that can come from thermal electrons, and high-amplitude noise, that may be caused by ion-induced pulses. The discriminator's output, observable on an oscilloscope, consists of uniform pulses of identical shape and magnitude, confirming the elimination of noise. The purified signal is routed to a counter, which records the number of photon detections (Channel A) over user-defined sampling intervals (Channel B). The latter is controlled by a secondary pulse generator, enabling a synchronization between light pulses and measurement windows. Data acquisition is automated via a PC, which aggregates counts for statistical analysis.

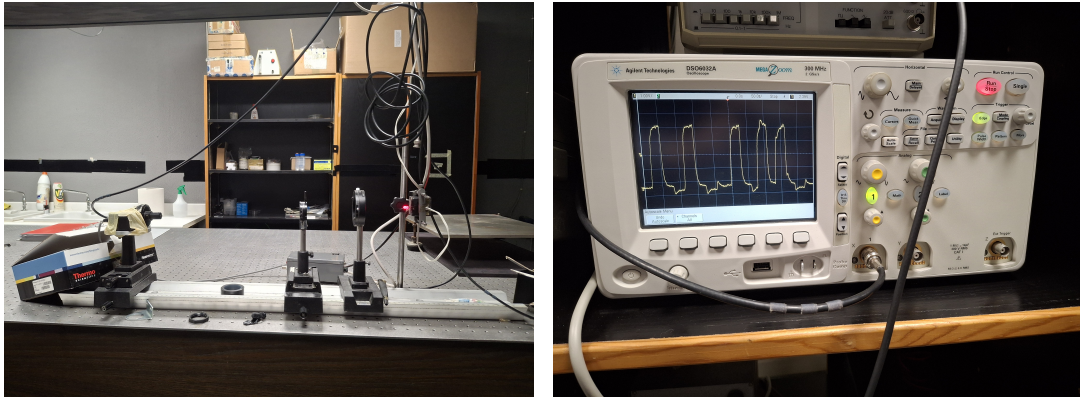


Figure 4: Images of the experimental setup used shown on Figure 3. To the left, the dark room, with the *LED*, the polarizers and the photomultiplier. To the right, the oscilloscope showing pulses.

To characterize the light's statistical behaviour, the experiment focused on determining the second-order factorial moment, $n^{(2)}$, as a function of the sampling time, T . For each T , ten independent measurements were performed, with each measurement integrating over 250 photon-counting cycles to minimize fluctuations. The LED's modulation factor, M , and the signal's period, P , were extracted by analysing the curve of $n^{(2)}$ as a function of T . A minimization algorithm was applied to fit the theoretical model to the empirical data, accounting for systematic effects such as detector dead time and pulse overlap.

3 Results and analysis

3.1 Validation of the theoretical model

Before proceeding with the collection of experimental data, it is essential to verify that the theoretical model describes the observed results. To achieve this, different values of the sampling parameter of the T/P ratio and the modulation factor M were selected, and the theoretical predictions were compared with the experimental measurements.

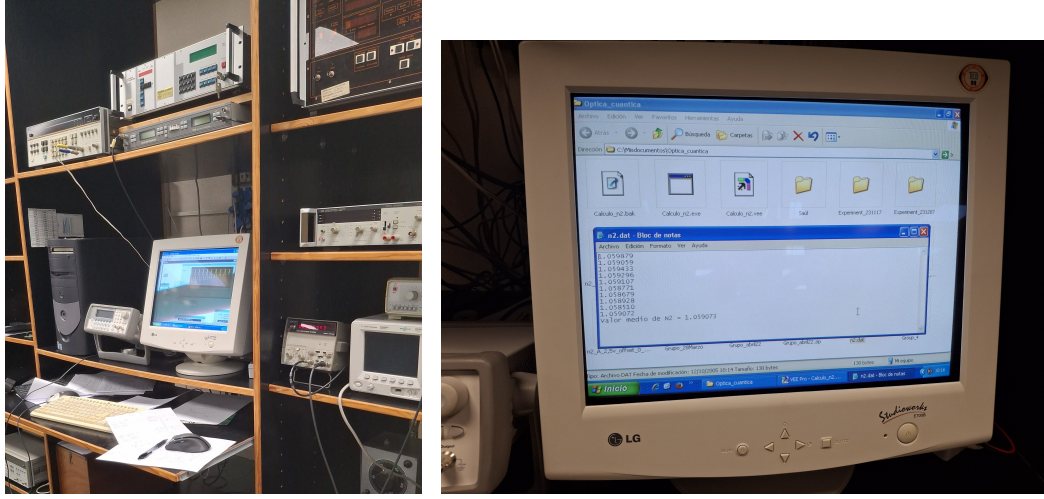


Figure 5: To the left, image of the experimental setup used shown on Figure 4. To the right, image of the data output given by the PC.

Table 1: Values of the characteristics of the test pulses including the T/P ratio and the modulation factor M . With them, the the theoretical values of the second order factorial moment, $n^{(2)}(T)_{theo}$, have been estimated, and experimental values, $n^{(2)}(T)_{exp}$, have been obtained. Finally, the relative deviation between both, δ_r .

	T/P	M	$n^{(2)}(T)_{theo}$	$n^{(2)}(T)_{exp}$	$\delta_r(n^{(2)}(T)) / \%$
test 1	0.01	1.00	1.98	1.970	0.5
test 2	0.3	1.00	1.60	1.596	0.25
test 3	0.3	0.73	1.32	1.326	0.45
test 4	0.7	0.73	1.06	1.059	0.09

The results in Table 1 indicate that, within the expected uncertainty range, the experimental values are consistent with the theoretical predictions. However, slight deviations were observed particularly when the sampling time was very low. This discrepancy may be attributed to increased statistical fluctuations. Since the theoretical predictions and experimental data match well, the setup works correctly, and the theoretical parameters can be used for further analysis.

3.2 Characterization of an unknown signal

In order to characterised the first unknown signal, for which we only know that the $M \neq 1$, first the values of the second order factorial moment for each sample time are taken, following the procedure explained:

Table 2: Experimental data obtained for the second order factorial moment for different sample time values, $n^{(2)}(T)$. The measurements were performed ten times for each sample time. The last two rows present the average values and the corresponding errors.

T / ms	$n^{(2)}(T)$									
	1	2	3	4	5	6	7	8	9	10
Series 1	1.209	1.191	1.151	1.113	1.074	1.051	1.0271	1.0128	1.0031	0.9999
Series 2	1.211	1.183	1.148	1.145	1.082	1.051	1.0271	1.0127	1.0035	0.9999
Series 3	1.210	1.188	1.137	1.090	1.071	1.051	1.0271	1.0127	1.0025	0.9999
Series 4	1.219	1.177	1.147	1.097	1.098	1.052	1.0275	1.0129	1.0024	0.9999
Series 5	1.224	1.182	1.155	1.098	1.022	1.051	1.0268	1.0128	1.0023	0.9999
Series 6	1.215	1.187	1.146	1.098	1.083	1.054	1.0274	1.0127	1.0033	0.9999
Series 7	1.213	1.191	1.158	1.092	1.092	1.051	1.0264	1.0126	1.0032	0.9999
Series 8	1.217	1.175	1.140	1.128	1.060	1.051	1.0273	1.0129	1.0023	0.9999
Series 9	1.224	1.183	1.149	1.086	1.072	1.050	1.0267	1.0129	1.0017	0.9999
Series 10	1.217	1.197	1.152	1.108	1.093	1.051	1.0262	1.0129	1.0023	0.9999
Average	1.216	1.186	1.149	1.106	1.08	1.0517	1.0270	1.01284	1.0027	0.999989
Error	0.005	0.006	0.005	0.018	0.02	0.0010	0.0004	0.00010	0.0006	0.000003

Using the obtained data, a preliminary estimation of the modulation factor, M , and the period P will be made by analysing the initial linear region of the curve obtained in the representation of the second factorial moment as a function of the sample time (Figure 6 on the left).

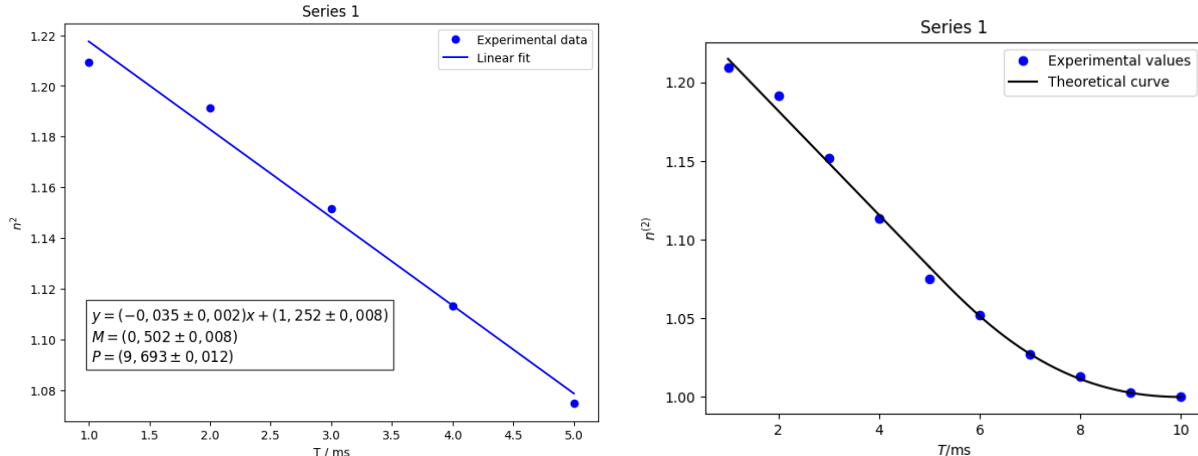


Figure 6: Representation obtained for the first series on Table 2. On the right, representation of the second order factorial moment as a function of the sample time in the initial linear region. On the left, representation of the minimization of the distance between theoretical and experimental values.

From the linear adjustment and with equation 4, the values of the modulation factor $M = 0.502 \pm 0.008$ and the period $P = 9.693 \pm 0.012$ ms have been estimated for the first series presented on Table 2. The Figure 6 on the right, illustrates the minimization of the difference between the experimental and theoretical values using a Python code, applied to the first series. This process has been repeated for the ten data series, obtaining ten estimated values of M and P and ten minimizations. Using a dataset of 250 samples, an optimization algorithm is implemented to determine the best-fit values for M and P . By iterating over the initial approximations obtained from the linear fit, the method ensures that the final values of M and P provide the best agreement with the measured data.

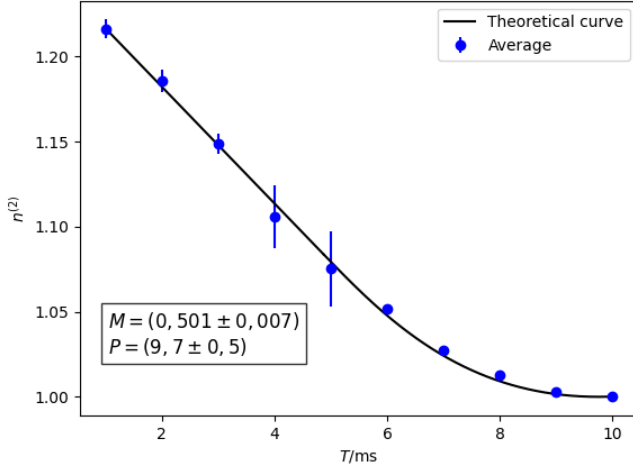


Figure 7: Representation of the second order factorial moment as a function of the sample time for the first set of measurements shown in Table 2.

Figure 7 illustrates the minimization of the difference between the experimental and theoretical values, applied to the full dataset in Table 2. Finally, a modulation factor of $\bar{M} = 0.501 \pm 0.007$ and $\bar{P} = 9.7 \pm 0.5$ ms were determined.

3.3 Characterization of a partially unknown signal

For this second measurement, the value of M has been changed, while the period P has remained the same. Therefore, we expect to obtain a P value similar to that of the previous signal.

Table 3: Experimental data obtained for the second order factorial moment for different sample time values, $n^{(2)}(T)$. The measurements were performed ten times for each sample time. The last two rows present the average values and the corresponding errors.

T / ms	$n^{(2)}(T)$									
	1	2	3	4	5	6	7	8	9	10
Series 1	1.455	1.402	1.347	1.252	1.172	1.112	1.060	1.030	1.006	0.999
Series 2	1.522	1.410	1.312	1.244	1.181	1.113	1.060	1.032	1.005	0.999
Series 3	1.476	1.405	1.335	1.266	1.183	1.113	1.059	1.032	1.005	0.999
Series 4	1.468	1.380	1.328	1.290	1.177	1.112	1.060	1.033	1.005	0.999
Series 5	1.510	1.384	1.365	1.283	1.179	1.111	1.060	1.033	1.005	0.999
Series 6	1.474	1.415	1.373	1.311	1.197	1.111	1.060	1.033	1.006	0.999
Series 7	1.475	1.414	1.264	1.351	1.189	1.117	1.062	1.032	1.006	0.999
Series 8	1.551	1.403	1.349	1.341	1.185	1.113	1.059	1.034	1.006	0.999
Series 9	1.399	1.375	1.244	1.313	1.176	1.114	1.059	1.033	1.007	0.999
Series 10	1.393	1.432	1.344	1.303	1.177	1.110	1.059	1.033	1.008	0.999
Average	1.47	1.403	1.33	1.30	1.182	1.1131	1.0603	1.0330	1.0064	0.999986
Error	0.05	0.017	0.04	0.03	0.007	0.0019	0.0008	0.0009	0.0011	0.000004

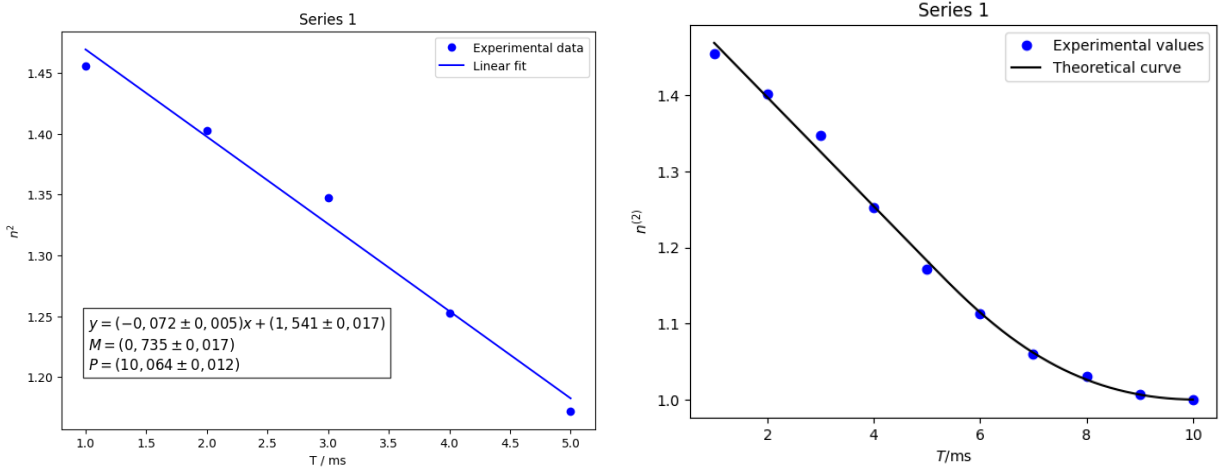


Figure 8: Representation obtained for the first series on Table 3. On the right, representation of the second order factorial moment as a function of the sample time in the initial linear region. On the left, representation of the minimization of the distance between theoretical and experimental values.

For this new set of measurements, values of $M = 0.735 \pm 0.017$ and $P = 10.064 \pm 0.012$ ms have been estimated for the first series. Then, using the previously mentioned Python code, the minimization process was performed again.

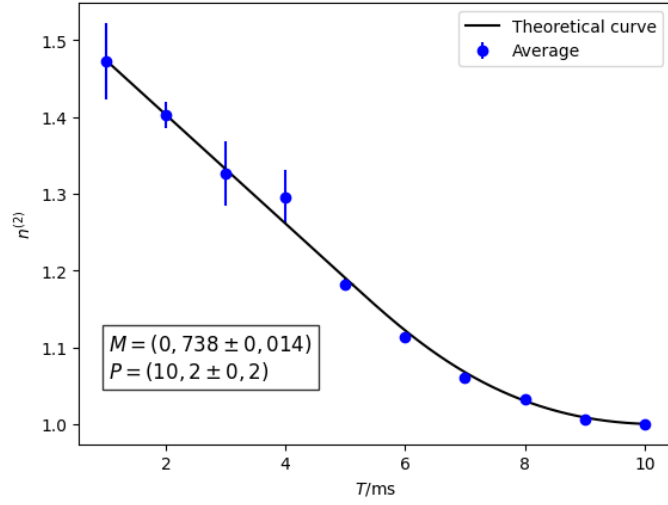


Figure 9: Representation of the second order factorial moment as a function of the sample time for the first set of measurements shown in Table 3.

Finally, the following values have been obtained: $\bar{M} = 0.738 \pm 0.014$ and $\bar{P} = 10.2 \pm 0.2$ ms.

4 Discussion

Once the results have been presented, it can be determined that, for the first signal (the unknown signal), the curve fitting for the second factorial moment in Figure 7 closely follows the experimental data, confirming that the theoretical model used in this experiment was correctly implemented and can be applied to similar signals in future analyses. In addition, values of $\bar{M} = 0.501 \pm 0.007$ and $\bar{P} = 9.7 \pm 0.5$ ms were determined. These results align with expectations, as during data collection, the signal became triangular upon reaching $T = 5$ ms. This suggests that at that point, the period can be estimated as $P = 2T$, meaning $P \approx 10$ ms. Additionally, the use of a minimization process to obtain the values of M and P helped reduce errors associated with variations in

the photomultiplier response.

As observed in the results in Table 2, at small sampling times, the deviation increases. This behaviour is expected since the second factorial moment provides information about the variability in the photon counting distribution. When the modulation factor is lower than one, the intensity fluctuations are more pronounced, leading to larger deviations at small sampling times. This occurs because, in such conditions, the number of detected photons is not sufficient to properly reconstruct the expected distribution. It is also important to consider that fluctuations in the signal can still introduce deviations. Increasing the number of samples would help reduce statistical noise but would not eliminate the intrinsic variability of the data.

Moreover, for the second signal (the partially unknown signal), the values obtained were $\bar{M} = 0.738 \pm 0.014$ and $\bar{P} = 10.2 \pm 0.2$ ms. Also, looking at Figure 9, the experimental data shows a poorer fit, especially around $T = 4$ ms. The P values are similar although they do not coincide, this could be due to any of the errors or fluctuations already mentioned.

5 Conclusions

The objectives of the experiment were achieved. First, fitting a function to experimental data was practised, helping to extract useful parameters and better understand the results. The importance of checking the experimental setup before starting measurements was also emphasized. Verifying that everything works correctly helps avoid errors and ensures reliable data collection.

Additionally, the experiment showed the value of using indirect measurements to determine parameters that cannot be measured directly. For example, in plasma physics, the temperature of a plasma cannot always be measured directly, but it can be inferred from the emitted radiation or the behaviour of charged particles. This method is widely used in physics to obtain information from related quantities.

References

- [1] F. González Fernández, "Analysis of a luminous signal with deterministic profile by using photon counting techniques". *Practice script*, 2019/20.

Appendix. A: Errors

In the case of the errors presented in tables 2 and 3 on the average of the measurements, as well as for the mean values of \bar{M} and \bar{P} , the standard deviation was used:

$$\sigma = \sqrt{\frac{\sum_i^N (x - \bar{x})^2}{N - 1}} \quad (6)$$

To obtain the errors in the estimates of P and M from Figures 6 and 8, error propagation was used:

$$\Delta P = \frac{4}{3} \sqrt{\left(\frac{\Delta m}{m^2} M^2\right)^2 + \left(\frac{2 \Delta M}{m} M\right)^2} \quad (7)$$

Appendix. B: Estimation of M and P

To obtain the estimated M and P values in both signals, a linear adjustment was made to the first points of the ten data series, obtaining 10 linear adjustments, described by the form: $y = a + bx$. Observing equation 4 it is easy to relate:

$$a = M^2 + 1$$

$$b = \left(-\frac{4T}{3P}\right)M^2$$

From these relations, the estimated values of M and P can be cleared and obtained with the adjustments obtained in Figures 6 and 8:

Table 4: Values obtained for P and M for every series of data on Table 2.

Serie	$M \pm \Delta M$	$P \pm \Delta P / \text{ms}$
1	0.502 ± 0.008	9.693 ± 0.012
2	0.493 ± 0.015	10.96 ± 0.03
3	0.503 ± 0.011	8.95 ± 0.02
4	0.495 ± 0.015	10.13 ± 0.02
5	0.532 ± 0.018	7.74 ± 0.03
6	0.502 ± 0.010	9.54 ± 0.02
7	0.502 ± 0.017	9.87 ± 0.03
8	0.503 ± 0.015	9.34 ± 0.02
9	0.514 ± 0.012	8.75 ± 0.02
10	0.505 ± 0.010	10.10 ± 0.02

Table 5: Values obtained for P and M for every series of data on Table 3.

Serie	$M \pm \Delta M$	$P \pm \Delta P / \text{ms}$
1	0.735 ± 0.017	10.064 ± 0.012
2	0.76 ± 0.02	9.267 ± 0.014
3	0.742 ± 0.005	10.142 ± 0.003
4	0.72 ± 0.02	10.515 ± 0.017
5	0.76 ± 0.03	10.02 ± 0.02
6	0.74 ± 0.03	11.173 ± 0.018
7	0.73 ± 0.07	11.14 ± 0.05
8	0.78 ± 0.05	10.15 ± 0.03
9	0.67 ± 0.06	11.94 ± 0.05
10	0.71 ± 0.05	11.86 ± 0.04